Exact nonequilibrium dynamics of finite-temperature Tonks-Girardeau gases

Y. Y. Atas,[1] D. M. Gangardt,[2] I. Bouchoule,[3] and K. V. Kheruntsyan[1]
[1]*University of Queensland, School of Mathematics and Physics, Brisbane, Queensland 4072, Australia*
[2]*School of Physics and Astronomy, University of Birmingham, Edgbaston, Birmingham B15 2TT, United Kingdom*
[3]*Laboratoire Charles Fabry, Institut d'Optique, CNRS, Univesité Paris Sud 11, 2 Avenue Augustin Fresnel, F-91127 Palaiseau Cedex, France*
(Received 20 December 2016; published 18 April 2017)

Describing finite-temperature nonequilibrium dynamics of interacting many-particle systems is a notoriously challenging problem in quantum many-body physics. Here we provide an exact solution to this problem for a system of strongly interacting bosons in one dimension in the Tonks-Girardeau regime of infinitely strong repulsive interactions. Using the Fredholm determinant approach and the Bose-Fermi mapping, we show how the problem can be reduced to a single-particle basis, wherein the finite-temperature effects enter the solution via an effective "dressing" of the single-particle wave functions by the Fermi-Dirac occupation factors. We demonstrate the utility of our approach and its computational efficiency in two nontrivial out-of-equilibrium scenarios: collective breathing-mode oscillations in a harmonic trap and collisional dynamics in the Newton's cradle setting involving real-time evolution in a periodic Bragg potential.

DOI: 10.1103/PhysRevA.95.043622

I. INTRODUCTION

Out-of-equilibrium phenomena are as prevalent in natural and engineered systems as equilibrium ones. Despite this, our understanding of nonequilibrium states of matter is far inferior to the understanding of equilibrium states governed by the broadly applicable foundational principles of statistical mechanics. In recent years, ultracold quantum gases have emerged as a platform of choice for studying nonequilibrium dynamics of interacting quantum many-body systems [1–6]. This is due to the fact that such gases represent nearly ideal and highly controllable realizations of various models of many-body theory in which such dynamics can be accessed on observable time scales. A particularly active area here concerned the study of quantum quenches and mechanisms of relaxation in one-dimensional (1D) Bose gases [7–11] (see also [4,12–17], and references therein), which, in the uniform limit, can be well approximated by the integrable Lieb-Liniger model [18] with δ-function pairwise interactions between the particles.

The limit of infinitely strong repulsive interactions in the Lieb-Liniger model corresponds to a 1D gas of impenetrable (hard-core) bosons, or the Tonks-Girardeau (TG) gas. The strong interactions required for realizing the TG gas have been achieved in ultracold-atom experiments in highly anisotropic traps [7,19–21], and its spectacular dynamics in a quantum Newton's cradle setting were observed in Ref. [7]. The particle impenetrability in the TG gas allows one to map the problem of many interacting bosons to an ideal (noninteracting) gas of fermions [22]. Remarkably, the Bose-Fermi mapping and hence the exact integrability of the model works not only in the uniform limit but also for inhomogeneous systems [23–25], which enables accurate tests of theory against experiments that are typically performed in harmonic traps. Despite this and despite the relatively long history behind the model, theoretical studies of TG gases have so far been limited to either zero- and finite-temperature *equilibrium* properties or *zero-temperature* dynamics [24,26–31]. *Finite-temperature dynamics*, on the other hand, is studied here and is important for accurate comparisons with experiments that are realized at nonzero temperatures.

In this work, we develop an exact finite-temperature dynamical theory of the TG gas applicable to arbitrary external potentials. More specifically, we propose a computationally efficient method for calculating the dynamics of single-particle density matrix and the corresponding momentum distribution of the gas. The method is based on the Fredholm determinant approach and the Bose-Fermi mapping, which allows one to solve the dynamical many-body problem in terms of the dynamics of single-particle quantities. This is similar to the zero-temperature approach of Ref. [27], except that we take into account finite-temperature effects. This results in an effective "dressing" of the single-particle wave functions by the square roots of Fermi-Dirac occupation factors. Our formalism is equally applicable to finite-temperature equilibrium calculations, in which case it offers significant computational advantages over the previously used approaches based on Lenard's formula [32–34]. For harmonically trapped systems, the efficiency of our approach is further unveiled by utilizing known analytic integrals and recurrence relations between Hermite polynomials.

II. ONE-BODY DENSITY MATRIX AND ITS EVOLUTION AT FINITE TEMPERATURE

A. Model Hamiltonian and Bose-Fermi mapping

We consider a 1D gas of N bosons of mass m, interacting via repulsive two-body δ-function potential and confined by a time-dependent one-body trapping potential $V(x,t)$ described by the Hamiltonian

$$\hat{H} = \sum_{j=1}^{N}\left[-\frac{\hbar^2}{2m}\frac{\partial^2}{\partial x_j^2} + V(x_j,t)\right] + g\sum_{j<l}\delta(x_j - x_l), \quad (1)$$

where $g > 0$ is the interaction strength. The infinitely strong contact interactions ($g \to \infty$) correspond to the TG gas of impenetrable bosons [18,22]. In this limit, the interactions are replaced by the hard-core constraints and the quantum many-body problem can be solved exactly.

Our goal is to study the real-time evolution of the one-body density matrix of the TG gas,

$$\rho(x,y;t) = \frac{1}{\mathcal{Z}} \sum_{N,\alpha} e^{\beta(\mu N - E_\alpha)} \int dx_2 \dots dx_N \times \Psi_\alpha(x,x_2,\dots,x_N;t)\Psi^*_\alpha(y,x_2,\dots,x_N;t). \quad (2)$$

Here, $\mathcal{Z} = \sum_{N,\alpha} e^{\beta(\mu N - E_\alpha)}$ is the grand-canonical partition function, $\beta \equiv 1/k_B T_0$, where T_0 is the initial equilibrium temperature, μ is the initial chemical potential, and $\Psi_\alpha(x_1,\dots,x_N;t)$ is the N-body wave function evolved according to the Schrödinger equation from the initial wave function $\Psi_\alpha(x_1,\dots,x_N;0)$.

At time $t = 0$, Eq. (2) describes the initial thermal equilibrium state of the system in the trapping potential $V(x,0)$ at temperature T_0. The density matrix allows one to calculate important observables, such as the real-space density $\rho(x,t) = \rho(x,x;t)$ and the momentum distribution $n(k,t) = \int dx\, dy\, e^{-ik(x-y)}\rho(x,y;t)$ of the gas.

The reduction of the many-body dynamical problem of a TG gas to a single-particle evolution relies on the existence of a Bose-Fermi mapping [22,24,25,35],

$$\Psi_\alpha(x_1,\dots,x_N;t) = A(x_1,\dots,x_N)\Psi^F_\alpha(x_1,\dots,x_N;t), \quad (3)$$

between the many-body wave functions Ψ_α of *interacting* (hard-core) bosons and those of *free* fermions, Ψ^F_α, where the function $A(x_1,\dots,x_N) = \prod_{1\leqslant j<i\leqslant N} \mathrm{sgn}(x_i - x_j)$ ensures the symmetrization of the bosonic wave functions.

The fermionic wave functions are constructed as Slater determinants, $\Psi^F_\alpha(x_1,\dots,x_N;t) = \det_{i,j=1}^N[\phi_{\alpha_i}(x_j,t)]/\sqrt{N!}$, of single-particle wave functions $\phi_{\alpha_i}(x,t)$ evolving according to the Schrödinger equation, with the initial wave functions $\phi_{\alpha_i}(x,0)$ being the eigenstates of the trapping potential $V(x,0)$, with eigenenergies E_{α_i} such that $E_\alpha = \sum_{i=1}^N E_{\alpha_i}$ and the index $\alpha = \{\alpha_1,\dots,\alpha_N\}$ representing the set of single-particle quantum numbers α_i that may occur.

As was shown by Lenard [32], the Bose-Fermi mapping allows one to express the one-body density matrix (2) in terms of the fermionic one-body density matrix,

$$\rho_F(x,y;t) = \sum_{i=0}^{\infty} f_i\, \phi_i(x,t)\phi^*_i(y,t), \quad (4)$$

which is a sum of products of single-particle wave functions weighted by the Fermi-Dirac occupation factors $f_i = [e^{(E_i-\mu)/k_B T_0} + 1]^{-1}$ for the ith single-particle orbital ($i = 0,1,\dots$) of energy E_i. The resulting expression for $\rho(x,y;t)$ can be expressed as an infinite series,

$$\rho(x,y;t) = \sum_{j=0}^{\infty} \frac{(-2)^j}{j!}[\mathrm{sgn}(x-y)]^j \times \int_x^y dx_2 \cdots dx_{j+1} \det_{k,l=1}^{j+1}[\rho_F(x_k,x_l;t)], \quad (5)$$

where in the determinant one has to take $x_k = x$ for $k = 1$ and $x_l = y$ for $l = 1$; the $j = 0$ term in the sum is given by $\rho_F(x,y;t)$ itself. In practice, it is difficult to use this formula for increasingly higher j (for example, in Ref. [33] only $j \leqslant 3$ terms were included in the calculated examples) as the large-j terms contain multiple (j-fold) integrals, in addition to entering the sum with alternating signs that lead to numerical inaccuracies.

B. Fredholm determinant approach to calculating the one-body density matrix

Here, we instead follow the approach of Refs. [36,37], which identified an alternative and more compact form of Lenard's formula, given by

$$\rho(x,y;t) = \det[1 - 2\hat{K}(t)]R(x,y;t), \quad (6)$$

i.e., a product of a Fredholm determinant and the associated resolvent operator $R(x,y;t)$ of the integral operator $\hat{K}$, whose action on an arbitrary function $g(r)$ is given by $(\hat{K}g)(w) = \int_x^y K(w,r;t)g(r)dr$, with the kernel $K(w,r;t) = \rho_F(w,r;t)$ in our case. The resolvent operator $R(x,y;t)$ satisfies the following integral equation [37]:

$$R(u,v;t) - 2\int_x^y K(u,r;t)R(r,v;t)dr = K(u,v;t). \quad (7)$$

Here, we have assumed $y \geqslant x$ without loss of generality and suppressed, for notational simplicity, the dependence of R on the integration limits, as the final results that we are interested in only depend on the values of R at $u = x$ and $v = y$. We point out that Eq. (5) corresponds to the expansion of the determinant in Eq. (6) by minors [36,38], and that a discrete version of Eq. (6) on a lattice has previously been obtained by Castin for a spatially homogeneous TG gas at $T = 0$ (see Eq. (3.37) in [39]).

At zero temperatures, the infinite sum appearing in the fermionic one-body density matrix (4), which also serves the role of the kernel K in Eq. (7), is effectively truncated by the highest occupied orbital term ($i = N - 1$) corresponding to the Fermi level. At finite temperatures, this is no longer true; however, for any practical calculation, the infinite series can be truncated at some large M beyond which the Fermi-Dirac occupancies are negligible. (In practice, the precise value of the cutoff M should be determined from the convergence properties of the final physical results of interest). Therefore, to a good approximation, the fermionic kernel in Eq. (7) can be replaced by a finite series $\rho_F(w,r;t) \simeq K_M(w,r;t) = \sum_{i=0}^M f_i\phi_i(w,t)\phi^*_i(r,t)$. Inserting this form of the kernel into Eq. (7) gives

$$R(u,v;t) = K_M(u,v;t) + 2\sum_{i=0}^{M} \sqrt{f_i}\phi_i(u,t)A_i(v;t), \quad (8)$$

where we have introduced the following notation:

$$A_i(v;t) = \sqrt{f_i}\int_x^y \phi^*_i(r,t)R(r,v;t)\,dr. \quad (9)$$

The functions $A_i(v;t)$ are determined as follows. Multiplying Eq. (8) by $\sqrt{f_j}\phi^*_j(u,t)$ and integrating on $[x,y]$, we obtain

$$A_j(v;t) = \sum_{i=0}^{M} S_{ji}(t)[\sqrt{f_i}\phi^*_i(v,t) + 2A_i(v;t)], \quad (10)$$

where the matrix elements $S_{ij} = (\mathbf{S})_{ij}$ are given by

$$S_{ij}(t) = \mathrm{sgn}(y-x)\sqrt{f_i f_j}\int_x^y \phi_i^*(x',t)\phi_j(x',t)\,dx', \qquad (11)$$

and where we again suppressed the dependence of $S_{ij}(t)$ on the integration limits.

We proceed by writing the equation satisfied by the functions A_i in a more compact matrix form. By writing the left-hand side of Eq. (10) as $A_j(v;t) = \sum_{i=0}^{M}\delta_{ji}A_i(v;t)$, we obtain

$$\sum_{i=0}^{M}[\delta_{ji} - 2S_{ji}(t)]A_i(v;t) = \sum_{i=0}^{M} S_{ji}(t)\sqrt{f_i}\phi_i^*(v,t). \qquad (12)$$

Introducing the vectors $\vec{A} = (A_0,\ldots,A_M)^{\mathsf{T}}$ and $\vec{\Phi} = (\sqrt{f_0}\phi_0^*,\ldots,\sqrt{f_M}\phi_M^*)^{\mathsf{T}}$, this can be rewritten as a matrix equation, $[\mathbb{1} - 2\mathbf{S}(t)]\vec{A}(v;t) = \mathbf{S}(t)\vec{\Phi}(v,t)$, which in turn can be inverted to yield $\vec{A}(v;t) = [\mathbb{1} - 2\mathbf{S}(t)]^{-1}\mathbf{S}(t)\vec{\Phi}(v,t)$. Inserting this expression into Eq. (8) and rewriting the fermionic kernel as a double sum, $K_M(u,v;t) = \sum_{i,j}[\sqrt{f_i}\phi_i(u,t)\,\delta_{ij}\sqrt{f_j}\phi_j^*(v,t)]$, we obtain that the resolvent operator $R(x,y;t)$ is given by

$$R(x,y;t) = \sum_{i,j=0}^{M}\sqrt{f_i}\,\phi_i(x,t)(\mathbb{1} - 2\mathbf{S}^{-1})_{ij}\sqrt{f_j}\,\phi_j^*(y,t). \qquad (13)$$

The Fredholm determinant that appears in the definition of the one-body density matrix, given by Eq. (6), is equal to $\det(\mathbb{1} - 2\mathbf{S})$ in the truncated basis [38]. Therefore, the corresponding final expression for the one-body density matrix of a finite-temperature TG gas, after taking the limit $M \to \infty$, can be written as

$$\rho(x,y;t) = \sum_{i,j=0}^{\infty}\sqrt{f_i}\phi_i(x,t)Q_{ij}(x,y;t)\sqrt{f_j}\phi_j^*(y,t). \qquad (14)$$

Here, Q_{ij} are the matrix elements of the operator $\mathbf{Q}(x,y;t) = (\mathbf{P}^{-1})^{\mathsf{T}}\det\mathbf{P}$ (which is an $M\times M$ matrix in the truncated basis), with

$$P_{ij}(x,y;t) = \delta_{ij} - 2\,\mathrm{sgn}(y-x)\sqrt{f_i f_j}\int_x^y dx'\,\phi_i(x',t)\phi_j^*(x',t). \qquad (15)$$

Thus, we have reduced Eq. (6) to a simple double sum, which does not contain multiple integrals or sign-alternating terms present in Lenard's formula. At zero temperature, Eqs. (14) and (15) reduce to the results of Ref. [27] as the Fermi-Dirac distribution function in this case is given by a step function equal to 1 for orbitals with $i \leqslant N-1$, or 0 otherwise. At nonzero temperature, the orbital wave functions, as our results show, become "dressed" by the square roots of the Fermi-Dirac occupation factors, ensuring, e.g., that the correct real-space density $\rho(x,t) \equiv \rho(x,x;t) = \sum_{i=0}^{\infty} f_i|\phi_i(x,t)|^2$ is recovered.

Equations (14) and (15) are the main results of this paper, representing a compact and computationally practical recipe for calculating the time-dependent one-body density matrix of the TG gas. They reduce the problem of finding $\rho(x,y;t)$ to solving the time-dependent Schrödinger equation for the single-particle orbitals $\phi_j(x,t)$ and calculating the matrix elements $P_{ij}(x,y;t)$. At time $t = 0$, Eq. (14) describes the initial finite-temperature equilibrium one-body density matrix; in its present form, it offers a more efficient and accurate way of calculating $\rho(x,y;0)$ compared to the previous approaches [32,33].

C. Dynamics in a harmonic trap

The calculation of the one-body density matrix $\rho(x,y;t)$, given by Eq. (14), requires, in general, the evaluation of the overlap matrix elements $P_{ij}(x,y;t)$, given by Eq. (15), between the time-evolved wave functions $\phi_j(x,t)$, starting from the initial single-particle wave functions $\phi_j(x,0)$. For the special case of evolution in a time-dependent *harmonic* trap, $V(x,t) = m\omega(t)^2x^2/2$, the wave functions $\phi_j(x,0)$ are given by the well-known Hermite-Gauss orbitals, whereas the evolution under the single-particle Schrödinger equation can be solved using a scaling transformation [26,40], which in turn leads to

$$\rho(x,y;t) = \frac{1}{\lambda}\rho_0(x/\lambda, y/\lambda)e^{im\dot{\lambda}(x^2-y^2)/2\hbar\lambda}, \qquad (16)$$

where $\rho_0(x,y) = \rho(x,y;0)$ is the initial one-body density matrix. The scaling parameter $\lambda(t)$ is determined from the solution of the second-order ordinary differential equation (ODE), $\ddot{\lambda} = -\omega(t)^2\lambda + \omega_0^2/\lambda^3$, with the initial conditions $\lambda(0) = 1$ and $\dot{\lambda}(0) = 0$. For the quench of the trapping frequency considered above, this ODE acquires the form of the Ermakov-Pinney equation, $\ddot{\lambda} = -\omega_1^2\lambda + \omega_0^2/\lambda^3$, with the solution $\lambda(t) = [1 + \epsilon\sin^2(\omega_1 t)]^{1/2}$.

The scaling solution (16) enormously simplifies the calculation of $\rho(x,y;t)$ as Eq. (14) is used only once—for calculating the *initial* equilibrium density matrix $\rho_0(x,y)$ of a harmonically trapped TG gas. In this case, the elements of the overlap matrix $P_{ij}(x,y;0)$ are computed for the harmonic-oscillator eigenstates, $\phi_j(x) = e^{-x^2/2l_{\mathrm{ho}}^2}H_j(x/l_{\mathrm{ho}})/(\pi^{1/4}\sqrt{2^j\,j!\,l_{\mathrm{ho}}})$, where $H_j(\xi)$ is the Hermite polynomial of degree j ($j = 0,1,2,\ldots$) and $l_{\mathrm{ho}} = \sqrt{\hbar/m\omega_0}$ is the harmonic-oscillator length. One then computes the determinant of the initial overlap matrix $\mathbf{P}$ and inverts it in order to evaluate the matrix elements $Q_{ij}(x,y,0)$ appearing in Eq. (14).

In order to describe higher-temperature samples and larger total number of atoms N with this seemingly straightforward procedure, one needs to incorporate increasingly higher orbital wave functions in the double sum in Eq. (14). This, in turn, requires evaluation of the overlap integrals between highly excited states in Eq. (15). (For example, for our highest temperature and highest N samples, we used harmonic-oscillator excited states of up to $j = 400$.) As the highly excited states are fast oscillating functions in position space, brute-force numerical integration will result in computational difficulties.

To overcome these difficulties, we instead develop and compute the overlap matrix elements using an alternative approach. Namely, for the off-diagonal elements $P_{jk}(x,y;0)$ ($j \neq k$), we resort to a known analytic formula for the harmonic-oscillator eigenstates, given in the form of the following indefinite integral [41]:

$$\int\varphi_j(\xi)\varphi_k^*(\xi)d\xi = \frac{e^{-\xi^2}[H_{j+1}(\xi)H_k(\xi) - H_j(\xi)H_{k+1}(\xi)]}{2(k-j)\sqrt{2^{j+k}\pi\,j!\,k!}}, \qquad (17)$$

(j-k)

where $\xi \equiv x/l_{\rm ho}$ and $\varphi_j(\xi) \equiv \sqrt{l_{\rm ho}}\phi_j(x)$. This formula is much simpler to use, especially at higher temperatures and larger N, than the one based on a finite series of confluent hypergeometric functions used in Ref. [33].

For the diagonal elements $P_{jj}(x,y;0)$, no similar formula exists to the best of our knowledge; however, we find that these elements can be computed efficiently using the following recursive method. We define a sequence of functions $\{M_j(\xi)\}_{j=0,1,\ldots}$ containing the desired diagonal matrix elements in the form of indefinite integrals,

$$M_j(\xi) = \frac{\sqrt{\pi}}{2}\mathrm{erf}(\xi) - \frac{1}{2^j j!}\int e^{-\xi^2} H_j^2(\xi)d\xi, \qquad (18)$$

where $\mathrm{erf}(\xi)$ is the error function and $M_0(\xi) = 0$. Using the well-known recurrence relation for the Hermite polynomials, this yields

$$M_{j+1}(\xi) = M_j(\xi) + \frac{e^{-\xi^2}}{2^{j+1}(j+1)!}H_j(\xi)H_{j+1}(\xi). \qquad (19)$$

Equations (17)–(19) thus allow for an efficient computation of all (diagonal and off-diagonal) matrix elements of $P_{ij}(x,y;0)$ without performing explicit numerical integration of products of harmonic-oscillator wave functions.

III. EXAMPLES OF EVOLUTION OF THE TONKS-GIRARDEAU GAS FROM A THERMAL EQUILIBRIUM STATE

As an immediate application and illustration of the broad applicability of our approach, we use it to analyze two paradigmatic problems of current experimental and theoretical interest: (a) collective breathing-mode oscillations of a finite-temperature TG gas in a harmonic trap and (b) collisional dynamics in the Newton's cradle setting which involves real-time evolution in a periodic Bragg potential.

For the first application, we consider a TG gas initially in thermal equilibrium in a harmonic potential $V(x,0) = m\omega_0^2 x^2/2$ with the frequency ω_0. To invoke the breathing-mode oscillations, we use a confinement quench in which at $t = 0$ the trap frequency is instantaneously changed from the prequench value ω_0 to a new value ω_1; we characterize the quench strength by a dimensionless parameter $\epsilon = \omega_0^2/\omega_1^2 - 1$. Figure 1 shows the evolution of the density profile $\rho(x,t)$ and the momentum distribution $n(k,t)$ after a strong quench ($\epsilon = 35$), for $N = 16$ particles and a dimensionless initial temperature of $\theta_0 \equiv k_B T_0/N\hbar\omega_0 = 0.01$. As follows from the scaling solutions of Eq. (16), the dynamics of $\rho(x,t)$ consists of self-similar broadening and narrowing cycles occurring at the fundamental breathing-mode frequency of $\omega_B = 2\omega_1$. In contrast, the momentum distribution displays periodic broadening and narrowing cycles that occur at *twice* the rate of the oscillations of the *in situ* density profile. Unlike the breathing-mode oscillations of an ideal Fermi gas, the momentum distribution of the TG gas becomes narrow not only at the outer turning points of the classical harmonic-oscillator motion, when the *in situ* density profile is the broadest (here corresponding to time instances of $\omega_1 t = \pi/2 + \pi l$, with $l = 1,2,\ldots$), but also at $\omega_1 t = \pi l$ when the gas is maximally compressed. We refer to these points

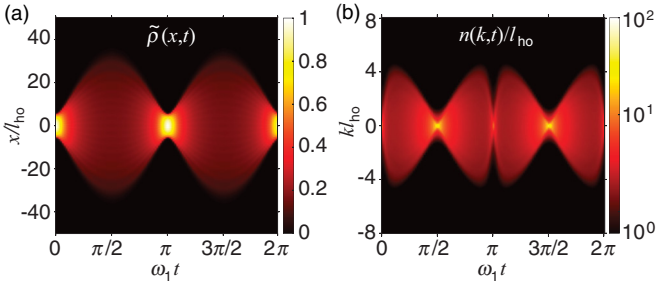

FIG. 1. Breathing-mode dynamics of the TG gas following a confinement quench. (a) Real-space density $\tilde{\rho}(x,t) \equiv \rho(x,t)/\rho(0,0)$ and (b) momentum distribution $n(k,t)/l_{\rm ho}$ (where $l_{\rm ho} = \sqrt{\hbar/m\omega_0}$ is the harmonic-oscillator length) as functions of the dimensionless time $\omega_1 t$, for $N = 16$ particles, quench strength $\epsilon = 35$, and dimensionless initial temperature $\theta_0 \equiv k_B T_0/N\hbar\omega_0 = 0.01$.

as the *inner* turning points, which serve as a manifestation of a collective many-body bounce effect due to the increased thermodynamic pressure of the gas that acts as a potential barrier. This phenomenon is similar to frequency doubling observed recently in a weakly interacting quasicondensate regime [11,42] and is further explored in Ref. [43].

As a second application of our approach, we analyze the dynamics of a finite-temperature TG gas in the Newton's cradle setting [7]. In this example (see Fig. 2), the initial atomic cloud in thermal equilibrium at temperature $\theta_0 = 0.1$ is subjected to a sequence of laser-induced Bragg pulses optimized to split the atomic wave packet into two counterpropagating halves corresponding to $\pm 2\hbar k_0$ diffraction orders of Bragg scattering [45]. This is modeled by a periodic lattice potential $V_{mB}(x,t) = \Omega(t)\cos(2k_0 x)$ of an amplitude $\Omega(t)$ (consisting

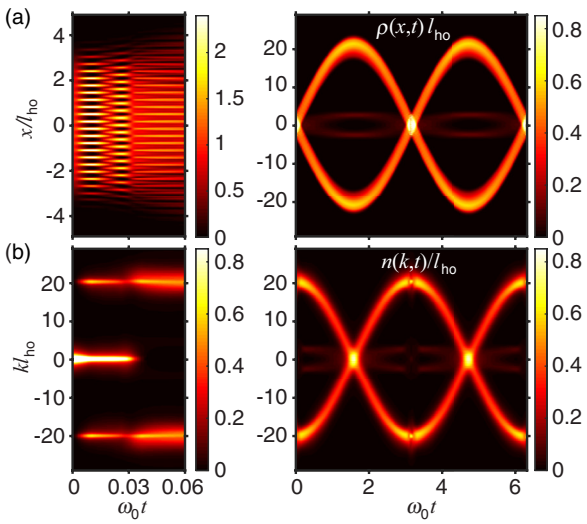

FIG. 2. Dynamics of the TG gas in the Newton's cradle setting. (a) The evolution of the real-space density, $\rho(x,t)l_{\rm ho}$, as a function of the dimensionless time $\tau = \omega_0 t$; the left panel is the magnified view into the time window containing the Bragg pulse sequence [44], whereas the right panel shows the full time window including post-Bragg periodic oscillations in the purely harmonic potential. (b) The respective momentum distribution, $n(k,t)/l_{\rm ho}$. In this example, $\theta_0 = 0.1$, $N = 5$, and $k_0 l_{\rm ho} = 10$.

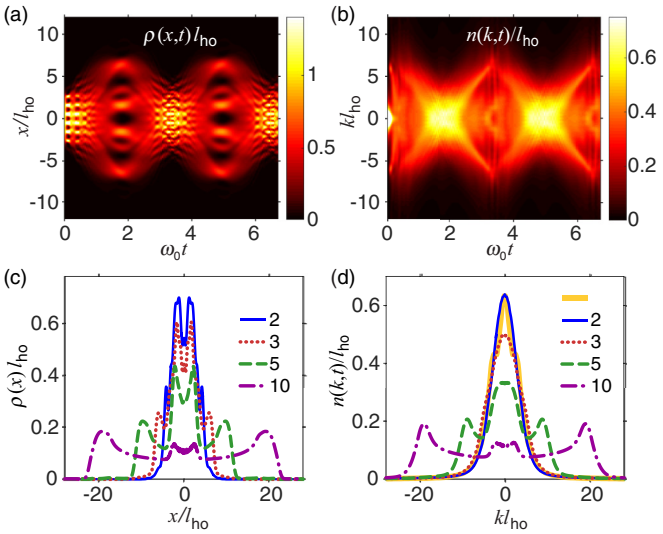

FIG. 3. (a),(b) Same as in the main panels of Fig. 2, but for $k_0 l_{ho} = 3$. (c),(d) The real-space density and momentum distributions averaged over a full oscillation period (as in Ref. [7]) starting immediately after the end of the Bragg pulse at time t_B, for $k_0 l_{ho} = 2,3,5,10$; in (d), the thick (light orange) solid line shows the momentum distribution $n(k,t_B)$, for $k_0 l_{ho} = 2$.

of two square pulses [44]), superimposed on top of the initial harmonic potential of frequency ω_0. Unlike the (short-pulse) Kapitza-Dirac regime of Bragg scattering analyzed, e.g., in Ref. [31], we operate in the (long-pulse) Bragg regime of the Newton's cradle experiment [7] wherein the interatomic interactions during the Bragg pulse are automatically taken into account, rather than neglected. The subsequent collisional dynamics of the gas in the underlying pure harmonic trap potential displays periodic behavior and the characteristic traits observed in [7].

In Fig. 3, we show the collisional dynamics under the same initial conditions, but for a smaller Bragg momentum. This is essentially equivalent to considering a higher-temperature sample and the same Bragg momentum as before: when the Bragg momentum becomes comparable to the initial thermal width of the momentum distribution, the Bragg pulse no longer splits the distribution into two well-defined peaks. As a result, we observe a rather distorted pattern of collisional oscillations, which nevertheless display the same periodicity as previously.

IV. SUMMARY

In conclusion, we have developed an exact finite-temperature dynamical theory of the Tonks-Girardeau gas applicable to arbitrary initial temperatures and trapping potentials, including arbitrary variations of the trapping potentials with time. The approach relies on the Fredholm determinant representation and the Bose-Fermi mapping, allowing one to reduce the problem of many-body evolution to a single-particle basis. For harmonically trapped gases, the approach further benefits from analytic scaling solutions for the single-particle wave functions, while for arbitrary trapping potentials the wave functions should be evolved numerically according to the single-particle Schrödinger equation. Our results open the way to systematic studies of nonequilibrium dynamics of this paradigmatic strongly interacting many-body system. The examples illustrated here concerned the breathing-mode oscillations and the Newton's cradle setup; however, other nonequilibrium scenarios can be easily considered, such as periodic driving, collisions in anharmonic traps, and formation of quantum shock waves, to name a few. In addition, our approach can be extended to treat finite-temperature dynamics of related integrable models, such as the XY spin model [46].

ACKNOWLEDGMENTS

The authors acknowledge fruitful discussions with Y. Castin, E. Bogomolny, and O. Giraud. Y.Y.A. thanks R. J. Lewis-Swan for the introduction to the XMDS software package used in the numerical simulations of the single-particle Schrödinger equation. I.B. acknowledges support by the Centre de Compétences Nanosciences Île-de-France. K.V.K. acknowledges support by the Australian Research Council Discovery Project, Grant No. DP140101763.

[1] I. Bloch, J. Dalibard, and W. Zwerger, Rev. Mod. Phys. **80**, 885 (2008).
[2] M. A. Cazalilla and M. Rigol, New J. Phys. **12**, 055006 (2010).
[3] A. Polkovnikov, K. Sengupta, A. Silva, and M. Vengalattore, Rev. Mod. Phys. **83**, 863 (2011).
[4] M. A. Cazalilla, R. Citro, T. Giamarchi, E. Orignac, and M. Rigol, Rev. Mod. Phys. **83**, 1405 (2011).
[5] A. Lamacraft and J. Moore, in *Ultracold Bosonic and Fermionic Gases*, Vol. 5 (Contemporary Concepts in Condensed Matter Science), edited by K. Levin, A. L. Fetter, and D. M. Stamper-Kurn (Elsevier, The Netherlands, 2012).
[6] J. Eisert, M. Friesdorf, and C. Gogolin, Nat. Phys. **11**, 124 (2015).
[7] T. Kinoshita, T. Wenger, and D. S. Weiss, Nature (London) **440**, 900 (2006).
[8] S. Hofferberth, I. Lesanovsky, B. Fischer, T. Schumm, and J. Schmiedmayer, Nature (London) **449**, 324 (2007).
[9] S. Trotzky, Y.-A. Chen, A. Flesch, I. P. McCulloch, U. Schollwöck, J. Eisert, and I. Bloch, Nat. Phys. **8**, 325 (2012).
[10] M. Gring, M. Kuhnert, T. Langen, T. Kitagawa, B. Rauer, M. Schreitl, I. Mazets, D. A. Smith, E. Demler, and J. Schmiedmayer, Science **337**, 1318 (2012).
[11] B. Fang, G. Carleo, A. Johnson, and I. Bouchoule, Phys. Rev. Lett. **113**, 035301 (2014).
[12] J.-S. Caux and R. M. Konik, Phys. Rev. Lett. **109**, 175301 (2012).
[13] D. Iyer and N. Andrei, Phys. Rev. Lett. **109**, 115304 (2012); D. Iyer, H. Guan, and N. Andrei, Phys. Rev. A **87**, 053628 (2013).
[14] M. Kormos, A. Shashi, Y.-Z. Chou, J.-S. Caux, and A. Imambekov, Phys. Rev. B **88**, 205131 (2013).

[15] J. De Nardis, B. Wouters, M. Brockmann, and J.-S. Caux, Phys. Rev. A **89**, 033601 (2014).
[16] J. C. Zill, T. M. Wright, K. V. Kheruntsyan, T. Gasenzer, and M. J. Davis, Phys. Rev. A **91**, 023611 (2015); New J. Phys. **18**, 045010 (2016).
[17] L. Piroli, P. Calabrese, and F. H. L. Essler, SciPost Phys. **1**, 001 (2016).
[18] E. H. Lieb and W. Liniger, Phys. Rev. **130**, 1605 (1963).
[19] T. Kinoshita, T. Wenger, and D. S. Weiss, Science **305**, 1125 (2004).
[20] B. Paredes, A. Widera, V. Murg, O. Mandel, S. Fölling, I. Cirac, G. V. Shlyapnikov, T. W. Hänsch, and I. Bloch, Nature (London) **429**, 277 (2004).
[21] E. Haller, M. Gustavsson, M. J. Mark, J. G. Danzl, R. Hart, G. Pupillo, and H.-C. Nägerl, Science **325**, 1224 (2009).
[22] M. Girardeau, J. Math. Phys. **1**, 516 (1960).
[23] M. D. Girardeau, Phys. Rev. **139**, B500 (1965).
[24] M. D. Girardeau and E. M. Wright, Phys. Rev. Lett. **84**, 5239 (2000).
[25] V. Yukalov and M. Girardeau, Laser Phys. Lett. **2**, 375 (2005).
[26] A. Minguzzi and D. M. Gangardt, Phys. Rev. Lett. **94**, 240404 (2005).
[27] R. Pezer and H. Buljan, Phys. Rev. Lett. **98**, 240403 (2007).
[28] M. Collura, S. Sotiriadis, and P. Calabrese, Phys. Rev. Lett. **110**, 245301 (2013).
[29] E. Quinn and M. Haque, Phys. Rev. A **90**, 053609 (2014).
[30] A. S. Campbell, D. M. Gangardt, and K. V. Kheruntsyan, Phys. Rev. Lett. **114**, 125302 (2015).
[31] R. van den Berg, B. Wouters, S. Eliëns, J. De Nardis, R. M. Konik, and J.-S. Caux, Phys. Rev. Lett. **116**, 225302 (2016).
[32] A. Lenard, J. Math. Phys. **7**, 1268 (1966).
[33] P. Vignolo and A. Minguzzi, Phys. Rev. Lett. **110**, 020403 (2013).
[34] Y. Hao, Y. Song, and X. Fu, Int. J. Mod. Phys. B **30**, 1650216 (2016).
[35] H. Buljan, R. Pezer, and T. Gasenzer, Phys. Rev. Lett. **100**, 080406 (2008).
[36] P. Forrester, N. Frankel, T. Garoni, and N. Witte, Commun. Math. Phys. **238**, 257 (2003).
[37] M. Jimbo, T. Miwa, Y. Môri, and M. Sato, Phys. D: Nonlin. Phenom. **1**, 80 (1980).
[38] F. Bornemann, Math. Comput. **79**, 871 (2010).
[39] Y. Castin, J. Phys. IV **116**, 89 (2004).
[40] A. Perelomov and Y. Zel'dovich, *Quantum Mechanics* (World Scientific, Singapore, 1998).
[41] J. C. Piquette, J. Symbol. Comput. **11**, 231 (1991).
[42] I. Bouchoule, S. S. Szigeti, M. J. Davis, and K. V. Kheruntsyan, Phys. Rev. A **94**, 051602 (2016).
[43] Y. Y. Atas, I. Bouchoule, D. M. Gangardt, and K. V. Kheruntsyan, arXiv:1612.04593.
[44] The overall Bragg pulse consists of two square pulses of duration $\tau_s = \pi/4\sqrt{2}\omega_B$ each, during which $\Omega(t) = 2\sqrt{2}\omega_B$ (with $\omega_B \equiv \hbar k_0^2/2m$), interrupted by a waiting interval of duration $\tau_{\rm wait} = \pi/4\omega_B$, during which $\Omega(t) = 0$ [45]; the overall duration of this double-Bragg pulse is $\tau_B = 0.0379$, after which the population is nearly completely transferred from the zero-centered momentum component into the $\pm 2\hbar k_0$ components.
[45] S. Wu, Y.-J. Wang, Q. Diot, and M. Prentiss, Phys. Rev. A **71**, 043602 (2005).
[46] E. Lieb, T. Schultz, and D. Mattis, Ann. Phys. **16**, 407 (1961).